Biogeosciences Discuss., 11, 17413–17462, 2014
www.biogeosciences-discuss.net/11/17413/2014/
doi:10.5194/bgd-11-17413-2014

Biogeosciences Discussions
Open Access

Autonomous profiling float observations of the high biomass plume downstream of the Kerguelen plateau in the Southern Ocean

M. Grenier[1,2], **A. Della Penna**[3,4,5,6], **and T. W. Trull**[4,1]

[1]Antarctic Climate and Ecosystems Cooperative Research Centre, Hobart, Tasmania, Australia
[2]Laboratoire d'Etudes en Géophysique et Océanographie Spatiales (LEGOS) (CNRS/CNES/IRD/University of Toulouse), Toulouse, France
[3]Quantitative Marine Sciences PhD Program, Institute for Marine and Antarctic Studies, University of Tasmania, Hobart, Tasmania, Australia
[4]Commonwealth Scientific and Industrial Research Organisation, Hobart, Tasmania, Australia
[5]Sorbonne Universités, UPMC Université Paris 06, UMR 7159, LOCEAN-IPSL, 75005, Paris, France
[6]Université Paris Diderot Cité, 5 rue Thomas-Mann, 75013 Paris, France

Received: 7 November 2014 – Accepted: 10 November 2014 – Published: 15 December 2014

Correspondence to: M. Grenier (melaniegrenier14@yahoo.fr)

Published by Copernicus Publications on behalf of the European Geosciences Union.

BGD
11, 17413–17462, 2014

Abstract

Natural iron fertilisation from Southern Ocean islands results in high primary production and phytoplankton biomass accumulations readily visible in satellite ocean colour observations. These images reveal great spatial complexity with highly varying concentrations of chlorophyll, presumably reflecting both variations in iron supply and conditions favouring phytoplankton accumulation. To examine the second aspect, in particular the influences of variations in temperature and stratification, we deployed four autonomous profiling floats in the Antarctic Circumpolar Current near the Kerguelen plateau in the Indian sector of the Southern Ocean. Each "bio-profiler" measured more than 250 profiles of temperature (T), salinity (S), dissolved oxygen, chlorophyll fluorescence (Chl *a*), and particle backscatter in the top 300 m of the water column, sampling up to 5 profiles per day along meandering trajectories extending up to 1000 km. Comparison of surface Chl *a* estimates (top 50 m depth; analogous to values from satellite images) with total water column inventories revealed largely linear relationships, suggesting that dilution of chlorophyll by mixed layer depth variations plays only a minor role in the spatial distributions observed by satellite, and correspondingly that these images provide credible information on total and not just surface biomass accumulations. Regions of very high Chl *a* accumulation (1.5–10 $\mu g\,L^{-1}$) were associated predominantly with a narrow T–S class of surface waters, which appears to derive from the northern Kerguelen plateau. In contrast, waters with only moderate Chl *a* enrichments (0.5–1.5 $\mu g\,L^{-1}$) displayed no clear correlation with water properties, including no dependence on mixed layer depth, suggesting a diversity of sources of iron and/or its efficient dispersion across filaments of the plume. The lack of dependence on mixed layer depth also indicates a limited influence on production by light limitation. One float became trapped in a cyclonic eddy, allowing temporal evaluation of the water column in early autumn. During this period, decreasing surface Chl *a* inventories corresponded with decreases in oxygen inventories on sub-mixed layer density surfaces, consistent with significant export of organic matter and its

BGD
11, 17413–17462, 2014

respiration and storage as dissolved inorganic carbon in the ocean interior. These results are encouraging for the expanded use of autonomous observing platforms to study biogeochemical, carbon cycle, and ecological problems, although the complex blend of Lagrangian and Eulerian sampling achieved by the floats suggests that arrays rather than single floats will often be required.

1 Introduction

The productivity of the Southern Ocean is important for many reasons. It supports fisheries and high conservation value marine mammal and bird populations (Constable et al., 2003; Nicol et al., 2000), influences the carbon dioxide content of the atmosphere (Sarmiento and Le Quéré, 1996; Sigman and Boyle, 2000; Watson et al., 2000), and affects the magnitude of nutrient supply to large portions of the global surface ocean (Sarmiento et al., 2004). This productivity is limited by the scarce availability of iron as an essential micro-nutrient (Boyd and Ellwood, 2010; Boyd et al., 2007; Martin, 1990). Island sources of Fe elevate productivity and produce downstream "plumes" of elevated phytoplankton biomass that contrasts with the general HNLC (High Nutrients, Low Chlorophyll) nature of the Southern Ocean (Blain et al., 2007; de Baar et al., 1995; Mongin et al., 2009; Pollard et al., 2009; Nielsdóttir et al., 2012). Ship based studies of several of these regions have mainly focused on determining the influence of Fe on C transfer to the ocean interior as part of understanding the role of these blooms' CO_2 absorption in the climate system (Blain et al., 2008; Salter et al., 2007), but in the process have revealed a complexity of responses in terms of intensity of enhanced productivity, biomass accumulation, and ecosystem structures. This diversity is the result of the interactions between the nature of the supply and bio-availability of iron, as well as variations in other drivers of productivity such as temperature, water column stratification and stability, light levels, and the possibility of co-limitation by other nutrients (Assmy et al., 2013; Boyd et al., 1999, 2001; Queguiner, 2013).

BGD
11, 17413–17462, 2014

This complexity is abundantly demonstrated by the "mosaic of blooms" encountered in waters downstream from the Kerguelen plateau during the KEOPS2 field program in austral spring (October–November 2011), as detailed in many papers in 2014 (d'Ovidio, 2014; Trull et al., 2014; Lasbleiz, 2014; Laurenceau et al., 2014; Cavagna et al., 2014). Much of the meso-scale spatial variations in biomass accumulation, as seen in satellite images and animations (Mongin et al., 2009; d'Ovidio, 2014; Trull et al., 2014), appears to result from the interleaving of iron-enriched water parcels that have transited the Kerguelen plateau with surrounding iron poor waters, as demonstrated by analysis of satellite altimetry based circulation estimates and surface drifter trajectories (Park et al., 2014; d'Ovidio, 2014). However, shipboard studies close to the plateau (Mosseri et al., 2008; d'Ovidio, 2014; Blain et al., 2014; Trull et al., 2014; Lasbleiz, 2014; Laurenceau et al., 2014) suggest that other factors also are likely to play a role, including mixed layer depth and upper water column stratification.

To explore the influence of variations in these water column properties on bloom structure at larger scale, in particular further from the plateau than could be surveyed by ship, we deployed autonomous profiling drifters. The first one was successfully launched during the KEOPS2 field program in late October 2011, and the other three during the MyctO-3D-MAP (referred to as MYCTO, from now on in this text) interdisciplinary survey in January 2014. Given the extent of the Kerguelen biomass plume (> 1000 km; Mongin et al., 2009), the remoteness from ports, and the presence of high waves and strong currents which preclude the navigation and recovery of other autonomous platforms, autonomous profilers were indeed the only way to obtain this information. As shown in Fig. 1, these deployments returned data from a large proportion of the enriched biomass plume downstream of the Kerguelen plateau.

In this paper, we use the bio-profiler observations to address three questions:

1. Do satellite images of surface chlorophyll provide an unbiased guide to the spatial distribution of total water column chlorophyll, or are they biased by lack of knowledge of the extent of deep mixing or the presence of subsurface chlorophyll maxima?

BGD
11, 17413–17462, 2014

2. Do regions of high biomass correlate with particular oceanographic properties, such as warmer or fresher waters, or the intensity of stratification? If so, are these properties determined locally or by the upstream origins of the different water parcels?

3. Can the fate of surface enrichments in biomass be determined from along-trajectory temporal variations in biogeochemical properties, for example by progressive downward movement of fluorescence or backscatter signals or decreases of oxygen in subsurface waters?

2 Methods

2.1 Float sensor and mission configurations

The float deployment locations, along with their identification numbers which provide access to their full data sets via the Australian Integrated Marine Observing System (www.imos.org.au), are provided in Table 1. The autonomous profiling floats were all of the same design (Model APF9I, Teledyne-Webb, Inc.). Each was equipped with pumped, poisoned, thermosalinographs (Model SBE 41CP-2., Seabird, Inc.), end-cap mounted unpumped oxygen optodes (Model 3830, Aanderaa, Inc.), and two-channel bio-optical sensors (Model FLBBAP2, Wetlabs, Inc.) strapped onto the lower third of the float hull with their optical ports facing horizontally to minimize possible interferences from particle accumulation. These sensors measure chlorophyll fluorescence by blue light stimulation and particle backscatter by red light scattering. Temperature and salinity calibrations were performed by Seabird, Inc., with estimated accuracy and precision of better than 0.005 °C and 0.01, respectively (Oka and Ando, 2004). The oxygen optodes were calibrated at CSIRO prior to mounting on the floats against a 20 point matrix of 4 temperatures (0.5–30) and 5 oxygen saturations (0–129 %) using the methods detailed in Weeding and Trull (2014). Similar sensors exhibited drift during a 6 month mooring deployment in the Southern Ocean of less than 1.7 µmol kg^{-1} over

BGD
11, 17413–17462, 2014

6 months (Weeding and Trull, 2014). The bio-optical sensors were measured against uranine solutions (with secondary scaling to a phytoplankton culture to roughly estimate chlorophyll concentrations; Wetlabs, Inc.) to calibrate linear responses with precisions of better than 10 %, and reproducibility for the set of three floats deployed in 2014 was found to be better than 4 % for values obtained by exposure to plastic covers made of fluorescent and non-reflective plastics (Earp et al., 2011). Owing to the structure of the firmware for the floats and the varying power requirements for the sensors, the sampling rates differed for the physical and biogeochemical parameters. Temperature and salinity were sampled at the highest rates, yielding values at 2 decibar intervals (used in this work as equivalent to 2 m depth intervals without density corrections); whereas oxygen, phytoplankton fluorescence, and particle backscatter were sampled at 10 decibar intervals.

In contrast to typical Argo program float missions for climate studies (www.argo.org), which consist of deep (2000 m) profiles every 10 days, the bio-profilers were programmed to focus on the upper water column and carried out continuous profiling between the surface and 300 m depth, achieving 4 to 6 profiles per day, depending on the stratification. This temporal resolution was intended to allow examination of daily cycles related to insolation, photosynthesis, and respiration. In practice, it proved difficult to extract clear cycles because of aliasing from spatial variations, and after several weeks for the 2011 KEOPS2 deployment of bio-profiler #1, the frequency of profiles was reduced to twice daily, to provide extended battery life while still obtaining night and day observations to allow insolation quenching of the fluorescence response to be evaluated, and thus to avoid inappropriate inference of subsurface chlorophyll maxima from the fluorescence signal (Sackmann et al., 2008; Xing et al., 2012). For bio-profilers #2, #3, and #4 deployed in 2014, the missions were further refined, via automated telemetric switching of mission configuration files, to carry out a deep profile to ∼ 1500 m every 3 days to provide deep reference points for temperature, salinity, and oxygen observations, and also with the intention to slow the development of bio-fouling of the bio-optical sensors by exposing surface organisms to high pressures.

BGD
11, 17413–17462, 2014

Float deployment was done in 2011 by manual transfer to a small boat and then the sea while the ship was on station, and in 2014 by lowering the floats from the ship deck inside cardboard boxes designed to readily disintegrate.

2.2 Float data quality control

As discussed in detail in the Results section below, the bio-profilers clearly provide an interesting and abundant source of measurements with which to examine correlations between biogeochemical and physical characteristics in the Kerguelen plume, but what is their level of fidelity? Are the values accurate, comparable, and free of temporal drifts? These are difficult questions to evaluate precisely, but some simple tests as summarized here, suggest that the data are reliable for our biogeochemical purposes, though more careful assessment against historical observations would be required for use in climate studies.

Extensive experience by the Argo program with profiling floats measurements for temperature and salinity, including recovery of floats for post deployment tests (Oka and Ando, 1994), suggests these sensors reliably deliver accurate and precise observations (to better than 0.005 °C and 0.01 salinity) over multi-annual deployments. Given our much shorter bio-profiler deployments and their observed T–S relationships which fall within those of the ship-based KEOPS2 observations, we assume these variables are correct and make no further assessments or corrections. We similarly accept the oxygen observations, given our careful attention to their pre-deployment calibration, their reasonable range of surface water oxygen super-saturations (96–103 % for low chlorophyll waters and extending up to 108 % in correlation with very high chlorophyll waters, as discussed further below), and their deep ocean values (950–1000 m depths) which fall within the range of nearby ship observations and showed no temporal trends and standard deviations of less than 4 umol kg^{-1} over the deployment periods (ranging from 1 to 3.9 umol kg^{-1} for the four bio-profilers).

For the bio-optical variables, to evaluate the possibility of temporal drifts in sensor responses, we examined variations in mesopelagic (250–300 m) and deep water (950–

BGD
11, 17413–17462, 2014

1000 m) values, i.e. at depths where little signal was anticipated and most profiles reached steady background values (Fig. 2a). The backscatter and, to a lesser extent, the fluorescence signals showed spikes which presumably reflect larger particles such as aggregates and zooplankton, motivating our examination of average values over 50 m ranges (250–300 m and 950–1000 m depth layers) for the assessment of temporal drifts. As shown in Fig. 2a, for most of their deployment periods all four bio-profilers exhibited no significant temporal drift of these deep values, but with a few important exceptions. The most important exception was for bio-profiler #1, for which high and erratic values of fluorescence and backscatter began to occur after profile #300 both at depth (Fig. 2a) and throughout the water column (Fig. 3.1c and 1e). We consider this to be caused by bio-fouling and do not use this data in any subsequent analysis (this loss of signal fidelity was one of the motivations for including periodic deep profiles in the subsequent three bio-profiler deployments, as a means of retarding fouling). In addition, a few discrete values (indicated by black arrows in Fig. 2a), were considered unrealistic and these profiles were also not used further. In contrast, the high fluorescence chlorophyll values found in mesopelagic waters from profiles ~ #110 to ~ #160 along the bio-profiler #1 trajectory appear to be real and to reflect the deep extension of high biomass occurrence at this time, as discussed further below (see also Fig. 3.1c).

We also corrected our fluorescence signals for daytime quenching. This effect, which derives from the photo-inhibition of phytoplankton by an excess of light (maximum at midday), decreases surface fluorescence (Falkowski and Kolber, 1995; Kiefer, 1973), and, if uncorrected, can produce a false impression of subsurface maxima in fluorescence derived chlorophyll profiles. A selection of daytime profiles from the four bio-profilers are shown to illustrate this effect (Fig. 2b, left panels). To correct this bias, we applied the efficient method of Sackmann et al. (2008), which uses the backscattering signal as a relative reference. Below the depth of daytime quenching we determined the fluorescence to backscattering ratio (over the depth range where it was constant), and multiplied this ratio by the backscattering signal to extrapolate

BGD
11, 17413–17462, 2014

the fluorescence signal to the surface. This assumes that phytoplankton populations are not stratified within the density defined mixed layer. This works particularly well for deep mixed layers (we defined the mixed layer depth, MLD, as the depth where density increased by 0.2 kg m^{-3} relative to the density at 10 m; Park et al., 1998) which exhibit relatively constant fluorescence/backscatter ratios (to within ~ 10 %) in their subsurface portions. We also identified profiles where daytime fluorescence quenching penetrated below the MLD, but a region of uniform fluorescence/backscatter ratios could still be identified below the MLD and this value was used for the extrapolation (for less than 15 % of the total quenching corrected profiles). Finally, in less than 5 % of the daytime profiles, we could not identify a region of uniform fluorescence/backscatter and apply the quenching correction; consequently, these profiles were not used further. The greater spikiness of the backscatter profiles in comparison to those of fluorescence (as illustrated in Fig. 2b, right panels) means that this quenching correction introduces some noise into the daytime chlorophyll estimates. In principle this could be filtered or smoothed, but the low 10 m vertical resolution of the observations made this rather uncertain and so we have used the unfiltered observations throughout this paper (except in Fig. 6f below where we show median-filtered backscatter profiles for the sake of visual clarity). The effects of the quenching correction on our selected chlorophyll profiles are shown in Fig. 2b (middle panels), and summary statistics for all the profiles are provided in Table 2. Without the correction, more than 90 % of the daytime profiles exhibited a subsurface maximum exceeding 30 % of the surface value. After correction this was reduced to very similar levels to those observed in the night time profiles (of less than 50 %), indicating that the correction was largely successful. Notably, for the total data set, after quenching correction, less than 12 % of the profiles exhibited a deep maximum exceeding 100 % of the surface value (Table 2), and these profiles were primarily located in a restricted region near the Gallieni Spur, as discussed further in the Results section.

BGD
11, 17413–17462, 2014

2.3 Satellite data comparisons

To provide physical and biological context for the bio-profiler trajectories and the effectiveness of their sampling of high biomass waters downstream of Kerguelen, we compared them to satellite products. For estimates of surface chlorophyll concentrations we used the CLS SSALTO/DUACS 4 km daily product derived from NASA MODIS-Aqua and observations (Fig. 1), without modification for recent suggestions that this algorithm may underestimate chlorophyll based on observations in low chlorophyll waters south of Australia (Johnson et al., 2013). Bio-profiler trajectory comparisons to eddy circulations were based on expectations for geostrophic currents estimated from satellite altimetry using the multi-satellite global product Delayed Time Maps of Absolute Dynamic Heights (DT-MADT) developed by the CNES/CLS Aviso project (www.aviso.oceanobs.com). This product has 1 week temporal and 1/3° spatial resolutions, and was used to compute Lagrangian trajectories to produce a diagnostic for eddy retention (d'Ovidio et al., 2013; Fig. 7b). This diagnostic is a measure of how much time a synthetic water parcel has been recirculating within an eddy core. Long-lived and coherent eddies are characterised by the water parcels with high values of retention (measured in days passed since the water parcel has been entrained by the eddy), whereas recently formed eddies or eddies that exchange strongly with surrounding regions have low retention values.

3 Results

3.1 Coverage of the plume

The drifts of the bio-profilers provided coverage of a large portion of the elevated biomass plume (Fig. 1), covering territory from near the Kerguelen plateau to more than 700 miles downstream (71 to 95° E) and nearly 400 miles from north to south (47.5 to 54° S), thereby spanning waters of the Polar Frontal and Antarctic Zones

BGD
11, 17413–17462, 2014

(Orsi et al., 1995; Park et al., 2008b; Sokolov and Rintoul, 2009). Unfortunately, this breadth of spatial coverage of the plume did not extend to full temporal seasonal coverage, and this is important to keep in mind given the strong seasonal cycle of biomass accumulation (Trull et al., 2014; Blain et al., 2007; Mongin et al., 2008). As shown in these images, the 2011 bio-profiler covered the period of highest biomass accumulation, while the 2014 deployments occurred after this seasonal peak, and thus sampled the system during its senescence. This provides some seasonal context for the central portion of the plume (which was sampled well in 2011 by bio-profiler #1 in spring and summer and again by bio-profilers #2 and #3 in summer and autumn). However, sampling of the north-eastern portion of the downstream plume (north of the Polar Front) was achieved only in late summer and autumn (by bio-profiler #4).

Bio-profiler #1 in spring 2011 and bio-profiler #3 in 2014 were deployed in the centre of the quasi-stationary cyclonic recirculation just east of the northern Kerguelen plateau (d'Ovidio, 2014; Park et al., 2014). Both bio-profilers exited this region to the northeast, tracking towards the Gallieni Spur, before transiting strongly southward near 74° E. This southward transport has also been observed for surface drifters and appears to be associated with a persistent meander of the Polar Front (d'Ovidio, 2014; Park et al., 2014). Thus bio-profilers #1 and #3 provide spring and summer perspectives respectively for these portions of the biomass plume (albeit in different years).

Bio-profiler #2 was deployed further south, close to the region where the strong north to south transport portions of the bio-profilers #1 and #3 trajectories finished. Thus bio-profiler #2 provided some overlap with the southern portion of the bio-profiler #1 trajectory, before being carried the furthest south, where it explored cold waters close to the Williams Ridge that extends to the southeast of Heard Island and terminates near the Fawn Trough (a gap in the plateau which permits the passage of much of the deep water eastward transport; Park et al., 2008b, 2014). Waters in this region tend to exhibit archetypical high-nutrient, low-chlorophyll characteristics, and were used as a reference station for iron non-fertilised waters during the KEOPS field program in 2005 (Blain et al., 2007, 2008).

BGD
11, 17413–17462, 2014

In contrast, bio-profiler #4 was deployed at similar latitude to bio-profilers #1 and #3, but further east, in particular east of the southward meander of the Polar Front which carried these others to the south. Bio-profiler #4 remained in the northern portion of the plume throughout its deployment, drifting to the northeast roughly parallel to the shallow Eastern Kerguelen Ridge before becoming trapped in a cyclonic eddy in which it obtained a time series of ∼ 100 profiles (as discussed in detail below).

3.2 Overview of observed oceanographic properties

The bio-profilers return a huge amount of water column data; each one provides more than most oceanographic voyages. Thus visualisation at the scale of individual profiles is only possible for targeted issues, and the simplest first-order assessment is most easily done by presenting the results as along-trajectory sections. These are shown for all the observed variables for each bio-profiler in Fig. 3, and briefly described in the following paragraphs.

Bio-profiler #1, launched in late October 2011 in the centre of the deep water recirculation just east of Kerguelen Island, initially encountered cold, fresh, well oxygenated waters with moderate biomass ($0.5\,\mu g\,L^{-1}$ < Chl *a* < $2\,\mu g\,L^{-1}$). It was then carried north-eastward across the Gallieni Spur where it encountered extremely high biomass (chlorophyll up to nearly $10\,\mu g\,L^{-1}$), which satellite ocean colour animations suggest was being swept northward as a mix of waters from the northern and central regions of the Kerguelen plateau (Trull et al., 2014). During the subsequent southward transport it crossed the Polar Front near 51.5° S, as shown by the presence of a temperature minimum near 150 m depth. The shoaling of low dissolved oxygen layers in this region provides another indication of their Antarctic Zone oceanographic classification. Surface waters above this remnant winter water were relatively warm (> 6 °C) despite deep mixed layer depths (∼ 100 m). Much of this warming is probably seasonal, as these waters were encountered in late summer, but the co-occurrence of somewhat elevated salinity suggests that flow of Polar Frontal Zone surface waters over the Antarctic waters was also involved. During the February bio-profiler transit, these

BGD
11, 17413–17462, 2014

waters exhibited only low to moderate chlorophyll biomass ($\sim 1.5\,\mu g\,L^{-1}$), although satellite images suggest higher concentrations ($\sim 3\,\mu g\,L^{-1}$) were present earlier in December and January (Trull et al., 2014). The particulate backscattering signal reflected the chlorophyll evolution along most of the trajectory, except in January when, as the high chlorophyll levels decreased, backscattering remained high and constant, suggesting detrital particles developed from the high chlorophyll biomass, or possibly a (relatively large) change in chlorophyll / particulate organic carbon ratio (Chl / POC) due to phytoplankton community composition. Finally, after 300 shallow profiles, bio-fouling of the fluorescence and backscatter sensors marks the end of their utility, as shown by the occurrence of elevated and highly noisy values throughout the water column (see Fig. 3.1c and 1e).

Bio-profiler #2, launched in late January 2014 south and east of the recirculation feature, initially encountered Polar Frontal Zone waters which were present further south in this region than during the 2011 year sampled by bio-profiler #1. For approximately the first 150 profiles these waters displayed relatively homogenous, moderately warm temperatures (4–5 °C) that continued to warm to ~ 6 °C through February. The bio-profiler then transited much further south, briefly encountering waters with strong shoaling of subsurface cold, salty, low oxygen characteristics near profile 160, and entered colder Antarctic waters where it remained through profile ~ 220, at which time its return north brought it back into Polar Frontal Zone waters showing autumn cooling. Throughout its life, in comparison to bio-profiler #1, only low-to-moderate biomass waters were encountered ($< 1.5\,\mu g\,L^{-1}$), though these values were persistently well above Southern Ocean HNLC background values ($< 0.6\,\mu g\,L^{-1}$). Within this range, the higher biomass values, which also extended over greater vertical extents, were found in the Antarctic waters. In contrast, the higher backscattering values were found at the beginning of the trajectory, and their deep extent and high values compared to chlorophyll levels suggest the existence of higher chlorophyll concentrations prior to the bio-profiler deployment. After this initial difference, the backscattering variations followed those of chlorophyll along the rest of the trajectory.

BGD
11, 17413–17462, 2014

Bio-profiler #3, launched in late January 2014 in the northern portion of the recirculation feature, followed a similar trajectory to that of bio-profiler #1 launched in October 2011, encountered much warmer waters with similar mixed layer depths, between 50 and 100 m. Presumably this represents seasonal warming as salinities were similar to those encountered in spring, and the warming ~3 to nearly 6 °C is consistent with seasonal warming amplitudes observed in satellite surface temperature records for unfertilized open ocean Polar Frontal Zone waters (Trull et al., 2001). Persistently higher chlorophyll levels were also observed initially in the recirculation region (up to ~4 vs. ~1 $\mu g\,L^{-1}$), but the float did not cross the Gallieni Spur where bio-profiler #1 encountered values up to nearly 10 $\mu g\,L^{-1}$. During its transit south near 74° E, only Polar Frontal Zone waters were encountered, and chlorophyll levels remained moderately high. At the beginning of the trajectory, the backscattering signal evolved in concert with the chlorophyll signal, but with a ~7–10 day delay. Another difference between the two biomass parameter evolutions was the large increase of particle backscatter compared to chlorophyll between the surface and 100 m, right after the profiler turned southward in the vicinity of the Gallieni Spur.

Bio-profiler #4, deployed well east of the recirculation feature in early February, was initially in warm, fresh and highly oxygenated waters, characterized by moderate biomass (first 80 profiles: chlorophyll $< 1.5\,\mu g\,L^{-1}$, $\log(b_{bp}) \sim 3.35\,m^{-1}$). Then, as its trajectory approached the Gallieni Spur, surface waters became progressively warmer, fresher and less oxygenated. During this time, the bio-profiler encountered a biomass rich filament, characterized by high and correlated chlorophyll and particle concentrations (chlorophyll values reaching up to 3 $\mu g\,L^{-1}$ for profiles 80–130). As it drifted further east it was entrained in a relatively stationary cyclonic eddy where it performed several loops before exiting to the south. This eddy can be identified from altimetry as retentive – i.e. capable of entraining Lagrangian particles for, in this case, a few weeks to one month (d'Ovidio et al., 2013; Fig. 7b). While retained by this mesoscale eddy, the bio-profiler measured a relatively constant profile of temperature and salinity, with slowly decreasing chlorophyll and backscatter concentrations (Fig. 7).

BGD
11, 17413–17462, 2014

Relatively constant hydrological properties throughout this period and the repeated looping suggest a largely Lagrangian trajectory within a single water parcel at this time. Of all the observations, this region displayed surface waters with the highest temperatures and lowest salinities.

4 Discussion

With this overview of the spatial and temporal characteristics of our observations in hand, we can proceed to evaluate our research questions.

4.1 Do the satellite images of surface chlorophyll reflect total inventories?

To evaluate this issue we did not compare our limited results to those from satellites (owing to only a small number of match-ups as limited by cloud cover), instead we considered our statistics on the occurrence of subsurface chlorophyll maxima (Table 2), which show that these features are relatively rare and localized. They occurred primarily near to the plateau and close to the location of the Polar Front (Fig. 4). Specifically, most of the profiles exhibiting this feature were found in the vicinity of the steep slope between the Northern Kerguelen Plateau and the Gallieni Spur, between 40 and 60 m depth. Occurrences of subsurface maxima were much more sporadic south of 50° S, on the south-eastward trajectories of bio-profilers #1 and #2. From this perspective, their presence is likely to lead to underestimation from satellite images of total chlorophyll inventories in this region. However, this effect is actually rather minor. To evaluate it we compared surface chlorophyll estimates from the bio-profilers with their total column inventories. For the surface estimates we used the average of the top 50 m in each profile (a depth which was within the mixed layer for the majority of the bio-profiler profiles and which represents ~2 e-folding depths for the satellite observations under conditions of low chlorophyll; we also calculated results for just the top 25 m, and found indistinguishable results). For the total column inventories we

BGD
11, 17413–17462, 2014

averaged down to 200 m (a depth below which negligible chlorophyll was observed). As shown in Fig. 5, the surface and total estimates show linear relationships over almost the entire range of observations, although the surface estimates are consistently higher than the total ones for chlorophyll concentrations higher than $1\,\mu g\,L^{-1}$. This suggests that variations in surface layer mixing, and the associated impact on the vertical distributions of chlorophyll, contribute insignificant bias where chlorophyll was low ($< 1\,\mu g\,L^{-1}$) but lead to over-estimation where chlorophyll was moderate to high ($> 1\,\mu g\,L^{-1}$). As such, satellite images tend to overestimate the dynamic range of total chlorophyll inventories, although this effect is relatively small, less than a factor of two even for surface chlorophyll concentrations as high as $10\,\mu g\,L^{-1}$. Given that our bio-profilers did not sample close to the plateau during the early summer peak in biomass as seen in satellite images, it is possible that there could be greater biases under these conditions. We also performed the same calculations for the backscatter signal, and found similar non-linearity, with negligible bias for surface backscatter values lower than $\sim 3.5\times10^{-4}\,m^{-1}$, and a significant bias towards higher estimates for surface values higher than this threshold value (where the slope breaks in the relationship between surface and total column backscatter, see Fig. 6). The origin of this non-linearity is not clear, and its evaluation is potentially compromised by the spikiness of the backscatter records and their poor vertical resolution, motivating refinement of bio-profiler firmware to allow achieve more frequent observations, potentially for subsets of profiles to retain reasonable mission duration.

4.2 Do regions of high biomass correlate with oceanographic properties?

To evaluate this issue we examined bivariate regressions of surface chlorophyll (top 50 m) with physical water column characteristics, after separation of the observations into two groups: (1) rich biomass regions close to the plateau, and (2) moderate biomass regions far from the plateau (see red and yellow rectangles in Figs. 3.1c, 3.2c, 3.3c and 3.4c). As shown in Fig. 6, the rich biomass regions encountered by bio-profiler #1 in 2011 and bio-profiler #3 in 2014 were associated with waters with

BGD
11, 17413–17462, 2014

very similar properties, specifically moderate temperatures (3.5–4.7 °C), high salinities (33.82–33.86), and thus relatively high densities (sigma-theta values of 26.8–27). The distributions of chlorophyll with these properties showed decreases on either side of these values, suggestive of mixing with surrounding waters. The origins of this particular class of waters is difficult to discern from our data, but based on surface drifter maps (d'Ovidio, 2014) appears to derive from the northern Kerguelen plateau. Thus this is an important target region for future studies of iron delivery mechanisms. For the moderate biomass observations, no clear relationships with mixed layer depth emerged (Fig. 6), suggesting a limited influence on production by light limitation, i.e. deep mixing was insufficient to lower light levels to limiting levels. But for the high biomass observations, there is a tendency for the highest chlorophyll concentrations to occur preferentially in shallow mixed layers, suggesting self-shading may become a limiting factor on production as biomass levels become very high (Fig. 6). This inference has been made previously from relationships between fluorescence and mixed layer depth observations in this region using sensors on elephant seals (Blain et al., 2013). Finally, for the highest chlorophyll profiles, mixed layer oxygen saturation states were as high as 8 %, exceeding levels expected from processes such as warming or bubble injection (Shadwick et al., 2014), and thus representing biological production.

4.3 Can the fate of surface enrichments in biomass be determined?

Evaluating this question requires the extraction of a temporal perspective from the bio-profiler records, and is thus only possible for portions of their trajectories which appear to be essentially Lagrangian. The best record for this approach is for bio-profiler #4 during the period when it carried out several clockwise loops in late autumn, i.e. for profiles 150–240 (Fig. 3.4a). During this time, its trajectory was very similar to that expected based on surface currents estimated from satellite altimetry, the density stratification of the water column was relatively steady, and the T–S profiles were tightly grouped (Fig. 7). These observations suggest that the profiler remained

BGD
11, 17413–17462, 2014

within a single water parcel, that was entrained by a retentive eddy and underwent only small exchanges with surrounding waters, as shown by slightly warmer (profiles 165–170 and 200–220) and cooler (profiles 175–195) conditions along the trajectory (these are discussed further below). At the start of this period, chlorophyll profiles showed elevated surface mixed layer levels, near 1.5 $\mu g L^{-1}$, and thus well above HNLC background values, with some profiles exhibiting subsurface maxima (Fig. 7e). The origin of these subsurface features is uncertain. One possibility is that they are remnants of the high surface chlorophyll biomass observed just prior to the eddy entrapment (Fig. 3.4c), that had been carried to depth by particle settling or by subduction of the denser, saltier, and slightly cooler water associated with that high biomass. After the start of the Lagrangian eddy entrapment period, the surface mixed layer chlorophyll levels declined further from 1.5 $\mu g L^{-1}$ to $< 1 \mu g L^{-1}$ (Fig. 3.4c and 7e). This decrease much exceeds the possible effect of dilution by mixed layer deepening of less than 10 %, and thus indicates chlorophyll conversion to non-fluorescent material, or its removal by export to depth or local respiration or both.

To evaluate these possibilities we examined changes in three layers, the surface layer (labelled layer 1 and defined as the surface down to the 26.6 isopycnal surface), and two density layers immediately below it (layers 2 and 3, respectively for density ranges 26.6–26.8 and 26.8–26.9). In order to characterize the existence of vertical or horizontal mixing during the eddy entrapment, mean temperature, salinity, depth of the density layers, as well as their thickness, are shown in Fig. 8 (a, b, and c). The thickness and mean depth of the surface density layer were relatively constant in the first half of the eddy entrapment, then slightly increased as some warmer and fresher – thus lighter – water entered into the eddy structure (profiles 200–220). Contrastingly, the physical properties of the two deeper underlying density layers showed insignificant temporal trends and smaller variability over the period of interest, and thus changes in their biogeochemical properties can be attributed to local processes rather than exchanges.

The evolution of chlorophyll, backscatter and dissolved oxygen inventories also exhibited different trends and variability for each layer (as shown in Fig. 8d, e, and f).

BGD
11, 17413–17462, 2014

In surface layer 1, mean chlorophyll and backscatter showed no overall temporal trend (green and grey curves in Fig. 8d, respectively), although characterized by two maxima, one at the beginning of the eddy and one coinciding with the fresher warmer water occurrence described above. The oxygen content continuously decreased steadily until after profile 200, when larger variations were observed, with a minimum content coinciding with the fresher warmer waters. Within the underlying layer 2, chlorophyll, backscatter and oxygen inventories showed similar evolutions: all had maximums at the beginning of the eddy and then decreased with time until the bio-profiler exited the eddy (Fig. 8e). These characteristics were also present in the deepest layer 3, although with significant differences in the magnitudes of change, specifically the oxygen decrease was similar to that of layer 2, but the chlorophyll level and its absolute magnitude of decrease were much smaller, and the backscatter levels remained relatively high for a longer portion of the record.

These variations suggest the following overall interpretation. In the surface layer 1, the chlorophyll inventory seems to result from the combination of local biological processes with weak horizontal resupply from warmer, fresher, and less oxygenated water (Fig. 7a and d). In the middle density layer 2, where mixing is considered insignificant because of the tightly grouped T–S properties, the chlorophyll decrease does not seem to be due to local transformation to non-fluorescent detritus since no corresponding increase in the backscatter signal was observed (Fig. 8e). This leaves loss by settling or respiration as possible explanations. Loss by settling is certainly possible on this timeframe (rates of only a few meters per day are required), and the high backscatter values found in the lower density layer 3 around profiles 160–180 could reflect transfer from the overlying layer 2. Biomass loss by respiration and remineralization to dissolved inorganic carbon is almost certainly also occurring given the decreasing oxygen inventories of the middle layer 2 and deep layer 3. For both these layers the rate of chlorophyll loss is too small (by factors of 2–3, assuming a moderately high phytoplankton C/Chl *a* ratio of 50) to explain all the oxygen decrease, implying that degradation of detritus (represented by the decreasing

BGD
11, 17413–17462, 2014

backscatter signal) and dissolved organic matter probably also contributes (this remains true even if we use a very high phytoplankton C/Chl *a* ratio of 100; Cloern et al., 1995). For the deepest layer 3, remineralization of settling particles coming from above with a minor remineralization of local chlorophyll may best explain the slower decrease of chlorophyll in comparison to that of oxygen.

In combination, these results suggest that not all of the accumulated biomass was respired in the surface layer, with the CO_2 then returned to the atmosphere, and thus that there was some sequestration. Quantifying the sequestration amount is difficult and merits a modelling and sensitivity assessment that is beyond the scope of this paper. Here we simply provide an indication of its possible magnitude by comparison of the rates of mean oxygen loss in the surface layer 1 (representing carbon likely to be returned to the atmosphere) vs. the subsurface layers 2 and 3 (representing carbon which may be sequestered in the ocean interior). The linear fits to the oxygen decreases for layers 1, 2, and 3 (as shown in Fig. 8) imply oxygen consumption rates of approximately 5, 4, and 4 $\mu mol\, m^{-3}\, d^{-1}$, respectively. These values lie towards the lower end of estimates for annual rates at mesopelagic depths (Sarmiento et al., 1990). Comparing O_2 consumption of layers 2 and 3 relative to the total mean consumption among the three layers, we estimate 40 % of the CO_2 produced during this autumn period of bloom decline was sequestered (25 % within layer 2 and 15 % within layer 3). An analogous area of low-to-moderate production and relatively high export was observed during the KEOPS2 field cruise just south of Polar Front, in a meander area around 72.5° E – 49° S where the flow – considered as Lagrangian – was sampled in few stations as a time series (Laurenceau et al., this issue; Planchon et al., this issue). This area coincides with the location of the anti-cyclonic trajectory of bio-profiler #3, around profile #110, where moderate biomass production was observed (Fig. 3.3c), although spatial variations in this region unfortunately precluded estimation of biologically driven oxygen consumption from the bio-profiler.

BGD
11, 17413–17462, 2014

5 Conclusions

The bio-profilers revealed several interesting aspects of the enriched biomass plume downstream from the Kerguelen plateau, by providing observations of its vertical dimension. First of all, the observations show that surface and total water column chlorophyll inventories are well correlated, which suggests that satellite perspectives on bloom spatial dynamics (e.g. Mongin et al., 2008, 2009) are unlikely to be strongly biased. This result holds true despite the presence of weak (30 % above surface values) subsurface chlorophyll maxima in ∼ 36 % of all the profiles, and strong (100 % above surface values) in ∼ 12 % of all the profiles (Table 2 and Fig. 4). However, half of these subsurface maxima were within the first 50 m depth, which corresponds to the depth range over which the surface data were integrated. That could partly explain why the magnitude of total chlorophyll still correlates well with surface chlorophyll even when subsurface maxima are present (Fig. 5). Our inference of lack of bias in satellite evaluations of the bloom spatial patterns does not mean that satellite chlorophyll estimates are necessarily accurate. That is an issue which our data cannot address owing to the imprecision of the bio-optical sensors and the absence of calibration against local chlorophyll observations, an approach which recent work has shown to be necessary (Johnson et al., 2013).

The occurrence of weak subsurface chlorophyll maxima in our data (∼ 36 % of all profiles) was higher than for results obtained with fluorescence sensors deployed on elephant seals around the Kerguelen plateau (< 9 %; Guinet et al., 2012) but lower than observed with other sets of autonomous floats elsewhere in the Southern Ocean (Carranza et al., 2014). This difference may reflect the greater proportion of observations in the southern portion of the plume in the Guinet et al. (2012) study, a region where we also found that subsurface maxima were uncommon (14 % of profiles for bio-profiler #2; Table 2). Subsurface maxima were also uncommon well downstream to the east of the Kerguelen plateau. This is interesting in that it suggests that subsurface iron levels supplied by upwelling or vertical mixing were insufficient

BGD
11, 17413–17462, 2014

to drive biomass accumulations at the base of the mixed layer, or at least were less important than horizontal supply of Fe in surface waters. This is in contrast to Polar Frontal Zone waters much further to the east south of Australia where persistent subsurface maxima have been observed (Parslow et al., 2001), and with observations from other autonomous profiling floats elsewhere in the Southern Ocean in which small subsurface maxima were found to be common in summer below the mixed layer (Carranza et al., 2014). Variations in the relative intensities of surface and deep iron supplies is a possible cause of these variations, but other processes may also be involved. As an example, the origin of the relatively more common and stronger subsurface chlorophyll maxima near the Gallieni Spur is not clear. Settling of surface biomass generated earlier in the season (Fig. 1) and/or seasonal depletion of iron in surface waters which reduces phytoplankton abundances are possibilities, but they cannot be assessed given our lack of early seasonal observations. A third possibility of the overlaying of low density waters southward across the Polar Front appears less likely, given that shipboard observations during KEOP2 found that this process generated shallow high biomass layers (at the Polar Frontal stations F-L, TEW-7, and TEW-8; Lasbleiz et al., 2014; Trull et al., 2014).

Our initial research goals included looking for oxygen production in deep chlorophyll maxima (Spitzer and Jenkins, 1989), but this could not be achieved owing to confounding effects on super-saturations from strong mixing with higher productivity overlying waters, and on apparent daily cycles from internal waves (Park et al., 2008a). Thus our results cannot address the issues of whether productivity in subsurface layers may partly explain offsets between satellite and in-situ estimates of the Southern Ocean biological pump (Schlitzer, 2002) or whether the phytoplankton that grow in deep chlorophyll maxima are preferential contributors to carbon export (Kemp et al., 2000; Queguiner, 2013). We were able to make a first simple assessment of subsurface autumn oxygen consumption during the portion of the bio-profiler #4 trajectory that delivered a quasi-Lagrangian time series, and this provided the very useful result that approximately 40 % of the biomass respiration in that period occurred beneath

BGD
11, 17413–17462, 2014

the mixed layer and thus under conditions favouring CO_2 sequestration in the ocean interior. This 40 % can be approximately equated to an export/production "*e* ratio" of 0.4, which is relatively high by global standards, but in the middle of the large range of values observed in cold Southern Ocean waters (Maiti et al., 2013), and similar to *f* ratios estimated for high biomass waters over the central Kerguelen plateau in autumn during the KEOPS1 campaign (Trull et al., 2008). Of course the subsequent fate of the sequestered CO_2 inferred from the bio-profiler #4 observations is uncertain, in that these waters were still within the depth range of possible exposure to the atmosphere during later deeper winter mixing, although the larger scale circulation in this region suggests it is a region dominated by subduction (Sallée et al., 2010).

Our simple correlative evaluation of the bio-profiler observations of biomass variations revealed that the highest chlorophyll levels were observed in surface waters with a narrow range of densities and moderate temperatures ($\sim 26.9 \pm 0.05$, $\sim 4 \pm 0.5\,^{\circ}C$; Fig. 6). This occurrence of maximum biomass at moderate temperatures, along with the lack of correlation with mixed layer depth (Fig. 6) suggests that local controls on growth rates were less important than the levels of iron supplied in this water type. Notably, water with these properties was found preferentially near the northern Kerguelen plateau and Gallieni Spur suggesting iron supply from this region. This is consistent with geostrophic circulation estimates and a favourable wind regime for upwelling in this region during the 2011 KEOPS2 period when bio-profiler #1 was deployed (d'Ovidio, 2014; Gille et al., 2014). Further observations and analysis are of course necessary to determine the generality of this inference that the northern Kerguelen plateau provides the major source of iron to the downstream biomass plume. This is especially true given the limited seasonal and inter-annual scope of our bio-profiler observations.

The Supplement related to this article is available online at doi:10.5194/bgd-11-17413-2014-supplement.

BGD
11, 17413–17462, 2014

Acknowledgements. This work was supported by the Australian Commonwealth Cooperative Research Program via the ACE CRC. M. Grenier was supported by a conjoint LEGOS and ACE CRC postdoctoral appointment. A. Della Penna was supported by a conjoint Frontières du Vivant (Paris 7) and CSIRO-UTAS Quantitative Marine Science PhD scholarship. We thank Ann Thresher (CSIRO) for the harvesting and processing of the data from the bio-profilers, as supported by the Australian Integrated Marine Observing Argo and Southern Ocean Time Series facilities. We thank Cedric Cotté and Francesco d'Ovidio (LOCEAN, Universite de Paris VI) and the crew of the *RV Marion Dufresne* for bio-profiler deployments, and Stephane Blain and Bernard Queguiner for KEOPS2 voyage leadership. Thanks to Vito Dirita, Alan Poole, and Craig Hanstein (CSIRO) for bio-profiler preparation, and Craig Neill and Kelly Brown (CSIRO) for oxygen optode calibrations. Thanks to Helen Phillips (IMAS) for fruitful discussions and advice concerning physical analyses of the hydrological variables, and Francesco d'Ovidio (University of Paris) for insights into Lagrangian perspectives on water parcel trajectories and their evolution.

References

Assmy, P., Smetacek, V., Montresor, M., Klaas, C., Henjes, J., Strass, V. H., Arrieta, J. M., Bathmann, U., Berg, G. M., and Breitbarth, E.: Thick-shelled, grazer-protected diatoms decouple ocean carbon and silicon cycles in the iron-limited Antarctic Circumpolar Current, P. Natl. Acad. Sci. USA, 110, 20633–20638, 2013.

Blain, S., Queguiner, B., Armand, L., Belviso, S., Bombled, B., Bopp, L., Bowie, A., Brunet, C., Brussaard, C., Carlotti, F., Christaki, U., Corbiere, A., Durand, I., Ebersbach, F., Fuda, J.-L., Garcia, N., Gerringa, L., Griffiths, B., Guigue, C., Guillerm, C., Jacquet, S., Jeandel, C., Laan, P., Lefevre, D., Lo Monaco, C., Malits, A., Mosseri, J., Obernosterer, I., Park, Y.-H., Picheral, M., Pondaven, P., Remenyi, T., Sandroni, V., Sarthou, G., Savoye, N., Scouarnec, L., Souhaut, M., Thuiller, D., Timmermans, K., Trull, T., Uitz, J., van Beek, P., Veldhuis, M., Vincent, D., Viollier, E., Vong, L., and Wagener, T.: Effect of natural iron fertilization on carbon sequestration in the Southern Ocean, Nature, 446, 1070–1074, doi:10.1038/nature05700, 2007.

BGD
11, 17413–17462, 2014

Blain, S., Queguiner, B., and Trull, T.: The natural iron fertilization experiment KEOPS (KErguelen Ocean and Plateau compared Study): An overview, Deep-Sea Res. Pt. II, 55, 559–565, doi:10.1016/j.dsr2.2008.01.002, 2008.

Blain, S., Renaut, S., Xing, X., Claustre, H., and Guinet, C.: Instrumented elephant seals reveal the seasonality in chlorophyll and light-mixing regime in the iron-fertilized Southern Ocean, Geophys. Res. Lett., 40, 052013, 1–5, doi:10.1002/2013GL058065, 2013.

Boyd, P., LaRoche, J., Gall, M., Frew, R., and McKay, R. L. M.: Role of iron, light, and silicate in controlling algal biomass in subantarctic waters SE of New Zealand, J. Geophys. Res., 104, 13395–13408, 1999.

Boyd, P. W., Crossley, A. C., DiTullio, G. R., Griffiths, F. B., Hutchins, D. A., Queguiner, B., Sedwick, P. N., and Trull, T. W.: Control of phytoplankton growth by iron supply and irradiance in the subantarctic Southern Ocean: experimental results from the SAZ Project, J. Geophys. Res., 106, 31573–31584, 2001.

Boyd, P. W., Jickells, T., Law, C. S., Blain, S., Boyle, E. A., Buesseler, K. O., Coale, K. H., Cullen, J. J., Baar, H. J. W. d., Follows, M., Harvey, M., Lancelot, C., Levasseur, M., Owens, N. P. J., Pollard, R., Rivkin, R. B., Sarmiento, J., Schoemann, V., Smetacek, V., Takeda, S., Tsuda, A., Turner, S., and Watson, A. J.: Mesoscale iron enrichment experiments 1993–2005: synthesis and future directions, Science, 315, 612–617, doi:10.1126/science.1131669, 2007.

Boyd, P. W. and Ellwood, M. J.: The biogeochemical cycle of iron in the ocean, Nat. Geosci., 3, 675–682, doi:10.1038/ngeo964, 2010.

Carranza, M. M., Gille, S. T., Franks, P. J. S., Girton, J. B., and Johnson, K. S.: Mixed-layer depth and Chl *a* variability in the Southern Ocean, ICES J. Mar. Sci., submitted, 2014.

Cloern, J. E., Grenz, C., and Vidergar-Lucas, L.: An empirical model of the phytoplankton chlorophyll: carbon ratio-the conservation factor between productivity and growth rate, Limnol. Oceanogr., 40, 1313–1321, 1995.

Constable, A. J., Nicol, S., and Strutton, P. G.: Southern Ocean productivity in relation to spatial and temporal variation in the physical environment, J. Geophys. Res., 108, 8079, doi:10.1029/2001JC001270, 2003.

d'Ovidio, F.: The biogeochemical structuring role of horizontal stirring: Lagrangian perspectives on iron delivery downstream of the Kerguelen plateau, Biogeosciences Discuss., submitted, 2014.

BGD
11, 17413–17462, 2014

d'Ovidio, F., De Monte, S., Della Penna, A., Cotté, C., and Guinet, C.: Ecological implications of eddy retention in the open ocean: a Lagrangian approach, J. Phys. A-Math. Theor., 46, 254023, doi:10.1088/1751-8113/46/25/254023, 2013.

de Baar, H. J. W., de Jong, J. T. M., Bakker, D. C. E., Loscher, B. M., Veth, C., Bathmann, U., and Smetacek, V.: Importance of iron for phytoplankton blooms and carbon dioxide drawdown in the Southern Ocean, Nature, 373, 412–415, 1995.

Earp, A., Hanson, C. E., Ralph, P. J., Brando, V. E., Allen, S., Baird, M., Clementson, L., Daniel, P., Dekker, A. G., and Fearns, P. R.: Review of fluorescent standards for calibration of in situ fluorometers: recommendations applied in coastal and ocean observing programs, Opt. Express, 19, 26768–26782, 2011.

Falkowski, P. G. and Kolber, Z.: Variations in chlorophyll fluorescence yields in phytoplankton in the world oceans, Aust. J. Plant Physiol., 22, 341–355, 1995.

Gille, S. T., Carranza, M. M., Cambra, R., and Morrow, R.: Wind-induced upwelling in the Kerguelen Plateau Region, Biogeosciences Discuss., 11, 8373–8397, doi:10.5194/bgd-11-8373-2014, 2014.

Guinet, C., Xing, X., Walker, E., Monestiez, P., Marchand, S., Picard, B., Jaud, T., Authier, M., Cotté, C., Dragon, A. C., Diamond, E., Antoine, D., Lovell, P., Blain, S., D'Ortenzio, F., and Claustre, H.: Calibration procedures and first dataset of Southern Ocean chlorophyll *a* profiles collected by elephant seals equipped with a newly developed CTD-fluorescence tags, Earth Syst. Sci. Data, 5, 15–29, doi:10.5194/essd-5-15-2013, 2013.

Johnson, R., Strutton, P. G., Wright, S. W., McMinn, A., and Meiners, K. M.: Three improved satellite chlorophyll algorithms for the Southern Ocean, J. Geophys. Res.-Oceans, 118, 1–10, 2013.

Kemp, A. E. S., Pike, J., Pearce, R. B., and Lange, C. B.: The "Fall dump" – a new perspective on the role of a "shade flora" in the annual cycle of diatom production and export flux, Deep-Sea Res. Pt. II, 47, 2129–2154, 2000.

Kiefer, D. A.: Fluoresence properties of natural phytoplankton populations, Mar. Biol., 22, 263–269, 1973.

Lasbleiz, M., Leblanc, K., Blain, S., Ras, J., Cornet-Barthaux, V., Hélias Nunige, S., and Quéguiner, B.: Pigments, elemental composition (C, N, P, and Si), and stoichiometry of particulate matter in the naturally iron fertilized region of Kerguelen in the Southern Ocean, Biogeosciences, 11, 5931–5955, doi:10.5194/bg-11-5931-2014, 2014.

BGD
11, 17413–17462, 2014

Laurenceau, E. C., Trull, T. W., Davies, D. M., Bray, S. G., Doran, J., Planchon, F., Carlotti, F., Jouandet, M.-P., Cavagna, A.-J., Waite, A. M., and Blain, S.: The relative importance of phytoplankton aggregates and zooplankton fecal pellets to carbon export: insights from free-drifting sediment trap deployments in naturally iron-fertilised waters near the Kerguelen plateau, Biogeosciences Discuss., 11, 13623–13673, doi:10.5194/bgd-11-13623-2014, 2014.

Maiti, K., Charette, M. A., Buesseler, K. O., and Kahru, M.: An inverse relationship between production and export efficiency in the Southern Ocean, Geophys. Res. Lett., 40, 1557–1561, 2013.

Martin, J. H.: Glacial–interglacial CO_2 change: the iron hypothesis, Paleoceanography, 5, 1–13, 1990.

Mongin, M., Molina, E., and Trull, T. W.: Seasonality and scale of the Kerguelen plateau phytoplankton bloom: a remote sensing and modeling analysis of the influence of natural iron fertilization in the Southern Ocean, Deep-Sea Res. Pt. II, 55, 880–892, doi:10.1016/j.dsr2.2007.12.039, 2008.

Mongin, M., Abraham, E. R., and Trull, T. W.: Winter advection of iron can explain the summer phytoplankton bloom that extends 1000 km downstream of the Kerguelen Plateau in the Southern Ocean, J. Mar. Res., 67, 225–237, 2009.

Nicol, S., Pauly, T., Vindoff, N., Wright, S., Thiele, D., Hosie, G., Strutton, P., and Woehler, E.: Ocean circulation off East Antarctica affects ecosystem structure and sea-ice extent, Nature, 406, 504–507, 2000.

Nielsdóttir, M. C., Bibby, T. S., Moore, C. M., Hinz, D. J., Sanders, R., Whitehouse, M. J., Korb, R. E., and Achterberg, E. P.: Seasonal and spatial dynamics of iron availability in the Scotia Sea, Mar. Chem., 130–131, 62–72, 2012.

Oka, E. and Ando, K.: Stability of temperature and conductivity sensors of Argo profiling floats, J. Oceanogr., 60, 253–258, 2004.

Orsi, A. H., Whitworth, T. I., and Nowlin, W. D. J.: On the meridional extent and fronts of the Antarctic Circumpolar Current, Deep-Sea Res., 42, 641–673, 1995.

Park, Y.-H., Fuda, J.-L., Durand, I., and Naveira Garabato, A. C.: Internal tides and vertical mixing over the Kerguelen Plateau, Deep-Sea Res. Pt. II, 55, 582–593, 2008a.

Park, Y.-H., Roquet, F., Fuda, J.-L., and Durand, I.: Large scale circulation over and around the Kerguelen Plateau, Deep-Sea Res. Pt. II, 55, 566–581, 2008b.

BGD
11, 17413–17462, 2014

Park, Y.-H., Charriaud, E., Ruiz Pino, D., and Jeandel, C.: Seasonal and interannual variability of the mixed layer properties and steric height at station KERFIX, southwest of Kerguelen, J. Marine Syst., 17, 571–586, 1998.

Park, Y.-H., Lee, J.-H., Durand, I., and Hong, C.-S.: Validation of the Thorpe scale-derived vertical diffusivities against microstructure measurements in the Kerguelen region, Biogeosciences Discuss., 11, 12137–12157, doi:10.5194/bgd-11-12137-2014, 2014.

Parslow, J., Boyd, P., Rintoul, S. R., and Griffiths, F. B.: A persistent sub-surface chlorophyll maximum in the Polar Frontal Zone south of Australia: seasonal progression and implications for phytoplankton-light-nutrient interactions, J. Geophys. Res., 106, 31543–31557, 2001.

Planchon, F., Ballas, D., Cavagna, A.-J., Bowie, A. R., Davies, D., Trull, T., Laurenceau, E., Van Der Merwe, P., and Dehairs, F.: Carbon export in the naturally iron-fertilized Kerguelen area of the Southern Ocean based on the ^{234}Th approach, Biogeosciences Discuss., 11, 15991–16032, doi:10.5194/bgd-11-15991-2014, 2014.

Pollard, R. T., Salter, I., Sanders, R. J., Lucas, M. I., Moore, C. M., Mills, R. A., Statham, P. J., Allen, J. T., Baker, A. R., Bakker, D. C. E., Charette, M. A., Fielding, S., Fones, G. R., French, M., Hickman, A. E., Holland, R. J., Hughes, J. A., Jickells, T. D., Lampitt, R. S., Morris, P. J., Nédélec, F. H., Nielsdóttir, M., Planquette, H., Popova, E. E., Poulton, A. J., Read, J. F., Seeyave, S., Smith, T., Stinchcombe, M., Taylor, S., Thomalla, S., Venables, H. J., Williamson, R., and Zubkov, M. V.: Southern Ocean deep-water carbon export enhanced by natural iron fertilization, Nature, 457, 577–580, doi:10.1038/nature07716, 2009.

Queguiner, B.: Iron fertilization and the structure of planktonic communities in high nutrient regions of the Southern Ocean, Deep-Sea Res. Pt. II, 90, 43–54, 2013.

Sackmann, B. S., Perry, M. J., and Eriksen, C. C.: Seaglider observations of variability in daytime fluorescence quenching of chlorophyll-*a* in Northeastern Pacific coastal waters, Biogeosciences Discuss., 5, 2839–2865, doi:10.5194/bgd-5-2839-2008, 2008.

Sallée, J.-B., Speer, K., Rintoul, S., and Wijffels, S.: Southern Ocean thermocline ventilation, J. Phys. Oceanogr., 40, 509–529, 2010.

Salter, I., Lampitt, R. S., Sanders, R., Poulton, A., Kemp, A. E. S., Boorman, B., Saw, K., and Pearce, R.: Estimating carbon, silica and diatom export from a naturally fertilised phytoplankton bloom in the Southern Ocean using PELAGRA: a novel drifting sediment trap, Deep-Sea Res. Pt. II, 54, 2233–2259, 2007.

BGD
11, 17413–17462, 2014

Sarmiento, J. L., Thiele, G., Key, R. M., and Moore, W. S.: Oxygen and nitrate new production and remineralization in the North Atlantic subtropical gyre, J. Geophys. Res.-Oceans, 95, 18303–18315, 1990.
Sarmiento, J. L. and Le Quéré, C.: Oceanic carbon dioxide uptake in a model of century-scale global warming, Science, 274, 1346–1350, 1996.
Schlitzer, R.: Carbon export fluxes in the Southern Ocean: results from inverse modeling and comparison with satellite-based estimates, Deep-Sea Res. Pt. II, 49, 1623–1644, 2002.
Shadwick, E. H., Trull, T. W., Tilbrook, B., Sutton, A., Schulz, E., and Sabine, C. L.: Seasonality of biological and physical controls on surface ocean CO_2 from hourly observations at the Southern Ocean Time Series site south of Australia, Global Biogeochem. Cy., in review, 2014.
Sigman, D. M. and Boyle, E. A.: Glacial/Interglacial variations in atmospheric carbon dioxide, Nature, 407, 859–869, 2000.
Sokolov, S. and Rintoul, S. R.: Circumpolar structure and distribution of the Antarctic Circumpolar Current fronts: 1. mean circumpolar paths, J. Geophys. Res., 114, C11018, doi:10.1029/2008JC005108, 2009.
Spitzer, W. S. and Jenkins, W. J.: Rates of vertical mixing, gas exchange and new production: Estimates from seasonal gas cycles in the upper ocean near Bermuda, J. Mar. Res., 47, 169–196, 1989.
Trull, T. W., Bray, S. G., Manganini, S. J., Honjo, S., and François, R.: Moored sediment trap measurements of carbon export in the Subantarctic and Polar Frontal Zones of the Southern Ocean, south of Australia, J. Geophys. Res., 106, 31489–31510, 2001.
Trull, T. W., Davies, D., and Casciotti, K.: Insights into nutrient assimilation and export in naturally iron-fertilized waters of the Southern Ocean from nitrogen, carbon and oxygen isotopes, Deep-Sea Res. Pt. II, 55, 820–840, doi:10.1016/j.dsr2.2007.12.035, 2008.
Trull, T. W., Davies, D. M., Dehairs, F., Cavagna, A.-J., Lasbleiz, M., Laurenceau, E. C., d'Ovidio, F., Planchon, F., Leblanc, K., Quéguiner, B., and Blain, S.: Chemometric perspectives on plankton community responses to natural iron fertilization over and downstream of the Kerguelen Plateau in the Southern Ocean, Biogeosciences Discuss., 11, 13841–13903, doi:10.5194/bgd-11-13841-2014, 2014.
Watson, A. J., Bakker, D. C. E., Ridgwell, A. J., Boyd, P. W., and Law, C. S.: Effect of iron supply on Southern Ocean CO_2 uptake and implications for glacial for atmospheric CO_2, Nature, 407, 730–733, 2000.

BGD
11, 17413–17462, 2014

Weeding, B. and Trull, T. W.: Hourly oxygen and total gas tension measurements at the Southern Ocean Time Series site reveal winter ventilation and spring net community production, J. Geophys. Res.-Oceans, 119, 348–358, doi:10.1002/2013JC009302, 2014.

Xing, X., Claustre, H., Blain, S., d'Ortenzio, F., Antoine, D., Ras, J., and Guinet, C.: Quenching correction for in vivo chlorophyll fluorescence acquired by autonomous platforms: a case study with instrumented elephant seals in the Kerguelen region (Southern Ocean), Limnol. Oceanogr.-Methods, 10, 483–495, 2012.

BGD
11, 17413–17462, 2014

Table 1. Bio-profiler deployments.

#	Hull#	WMO#	UTC Date	Lat. (°N)	Long. (°E)	Campaign
1	5122	1901329	29 Oct 2011	−48.5	72.2	KEOPS2
2	6684	5904882	26 Jan 2014	−49.9	76.2	MYCTO
3	6682	1901338	28 Jan 2014	−48.4	71.5	MYCTO
4	6683	1901339	4 Feb 2014	−48.6	74.0	MYCTO

BGD
11, 17413–17462, 2014

Table 2. Fluorescence quenching corrections and subsurface chlorophyll maxima statistics.

Individual bio-profiler statistics	1	2	3	4
Fluorescence profiles collected	384	298	278	254
Fluorescence profiles usable	300	298	277	254
Day time profiles	150	122	111	107
Night time profiles	150	176	166	147
Night time profiles with subsurface maxima[a] (percent of night time profiles)	68 (45 %)	16 (9 %)	74 (45 %)	54 (37 %)
Day time profiles with subsurface maxima[a] before correction (percent of daytime profiles)	138 (99 %)	96 (96 %)	106 (95 %)	98 (92 %)
Quenching corrected profiles	148	117	106	104
Day time profiles with subsurface maxima[a] before correction (percent of daytime profiles)	70 (47 %)	26 (22 %)	49 (46 %)	50 (48 %)
Day time profiles with correction below the mixed layer (percent of all corrected daytime profiles)	14 (9 %)	3 (3 %)	15 (14 %)	14 (13 %)
Total night and corrected day profiles with subsurface maxima[a] (% of night and corrected day profiles)	138 (46 %)	42 (14 %)	123 (45 %)	104 (41 %)
Total night and corrected day profiles with large subsurface maxima[b] (% of night and corrected day profiles)	39 (13 %)	6 (2 %)	28 (10 %)	51 (20 %)

[a] Subsurface values exceeding surface values by more than 30 %.
[b] Subsurface values exceeding surface values by more than 100 %.

BGD
11, 17413–17462, 2014

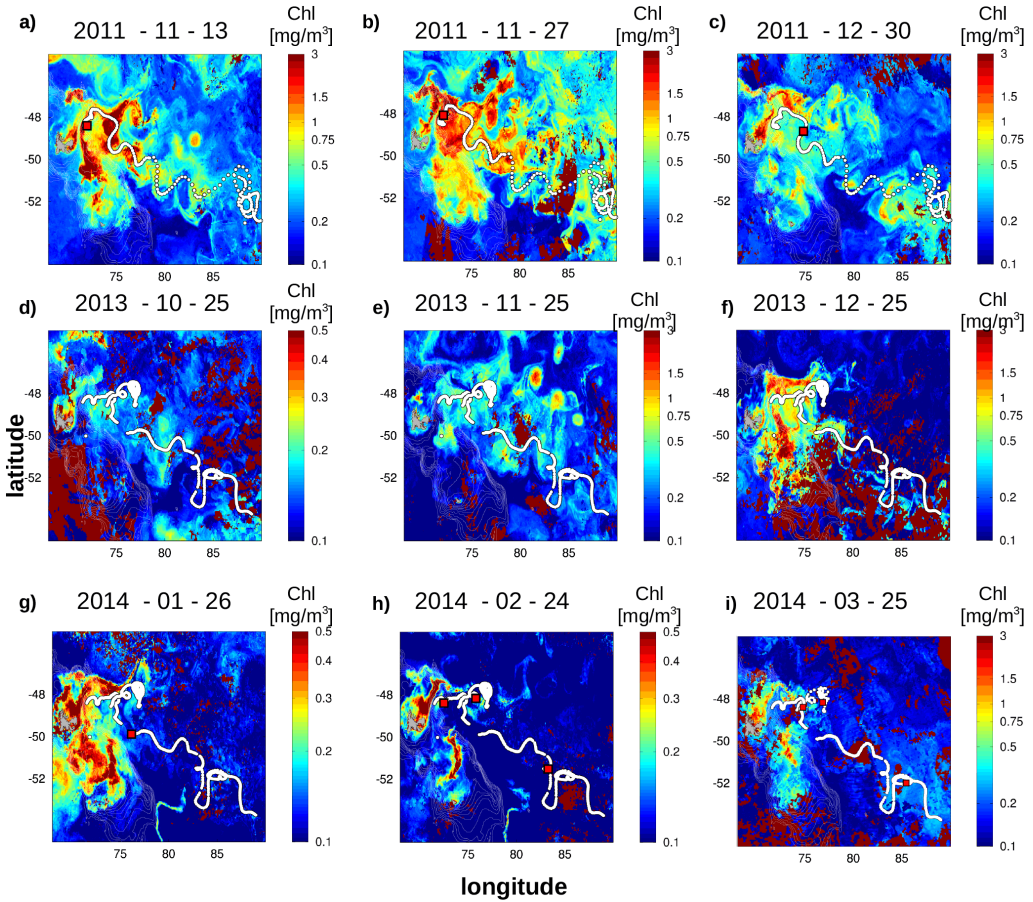

Figure 1. Bio-profiler trajectories (white lines) in comparison to satellite chlorophyll distributions. Top row: 2011 year for bio-profiler #1. Middle and bottom rows: 2013/14 year for bio-profilers #2, 3, 4. Red squares show bio-profiler locations on image dates.

BGD
11, 17413–17462, 2014

Autonomous profiling float observations of high biomass plume

M. Grenier et al.

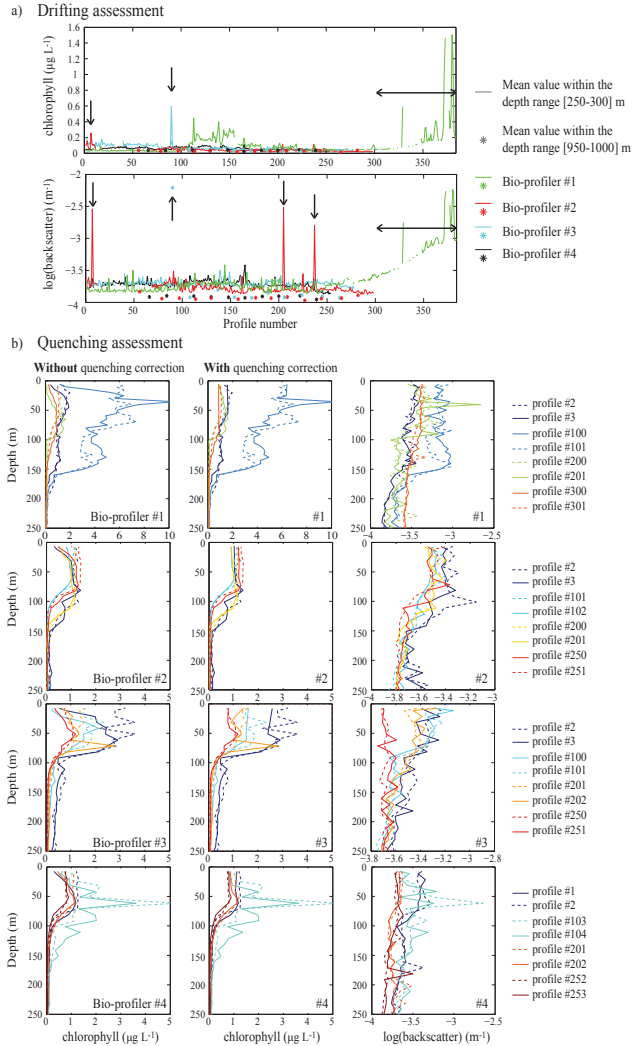

BGD
11, 17413–17462, 2014

Autonomous profiling float observations of high biomass plume

M. Grenier et al.

Figure 2. (a) Assessment of bio-optical sensor stability from temporal evolution of the mean chlorophyll and backscatter values within two depth ranges, 250–300 m (lines) and 950–1000 m (stars), for the 4 bio-profilers. Arrows indicate discrete profiles or ranges of profiles considered to be affected by bio-fouling, and were not used in further analysis. **(b)** Illustration of quenching corrections, showing pairs of successive day/night or night/day profiles (day: continuous lines; night: dashed lines). For each bio-profiler, the panels show: chlorophyll profiles without quenching correction (left), chlorophyll profiles with quenching correction (middle), and associated backscatter profiles (right).

BGD
11, 17413–17462, 2014

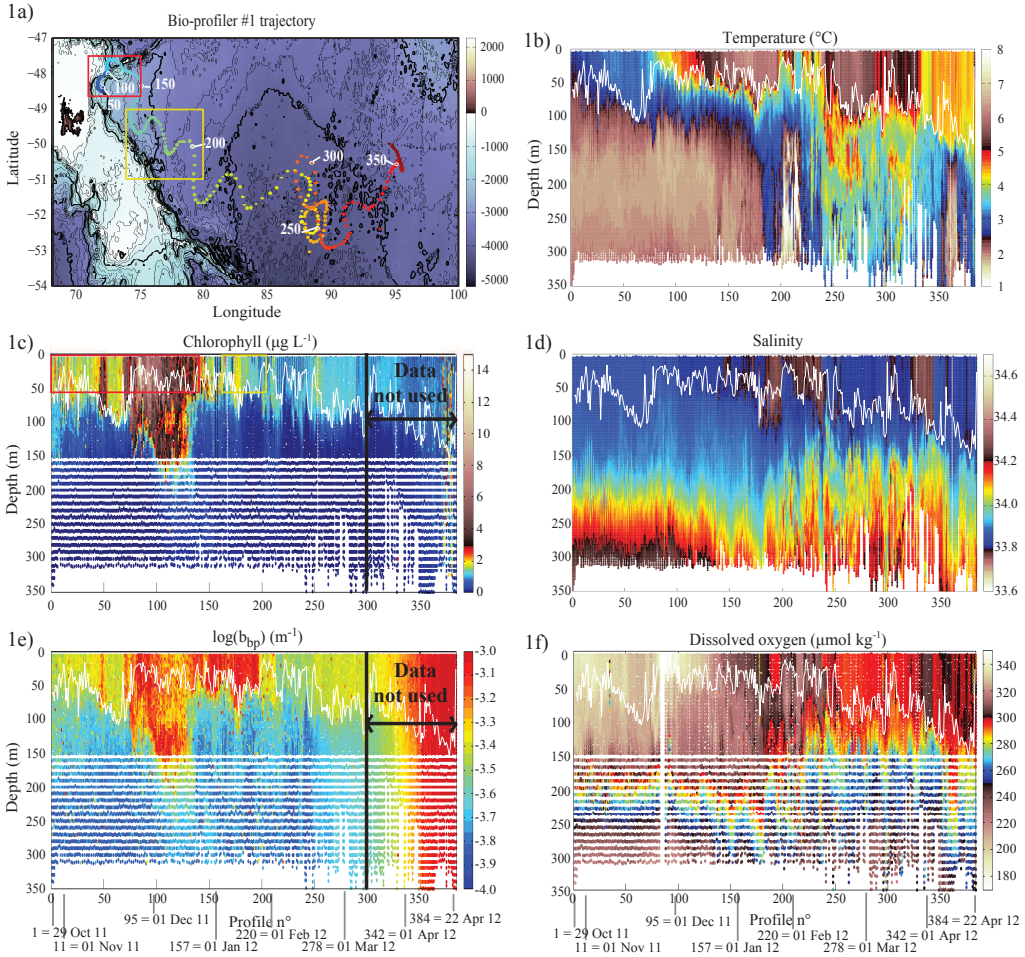

Figure 3.

BGD
11, 17413–17462, 2014

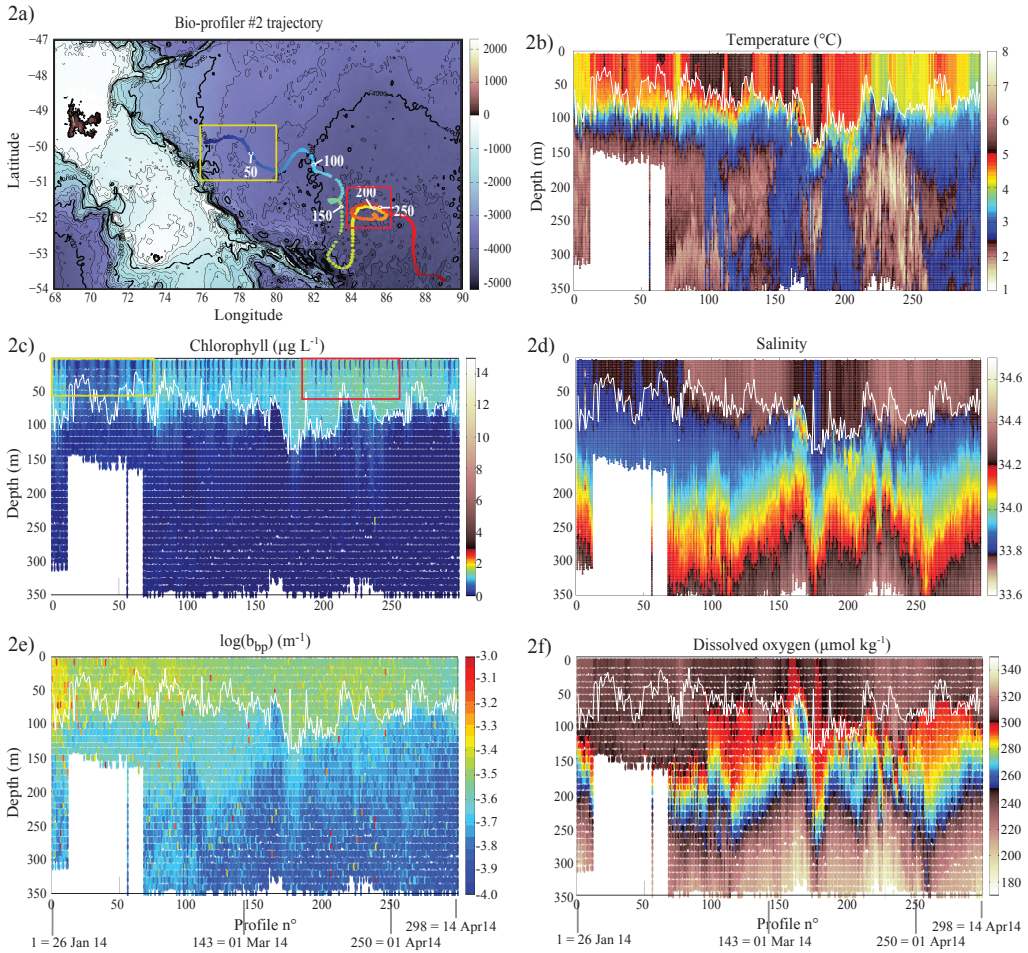

Figure 3.

BGD
11, 17413–17462, 2014

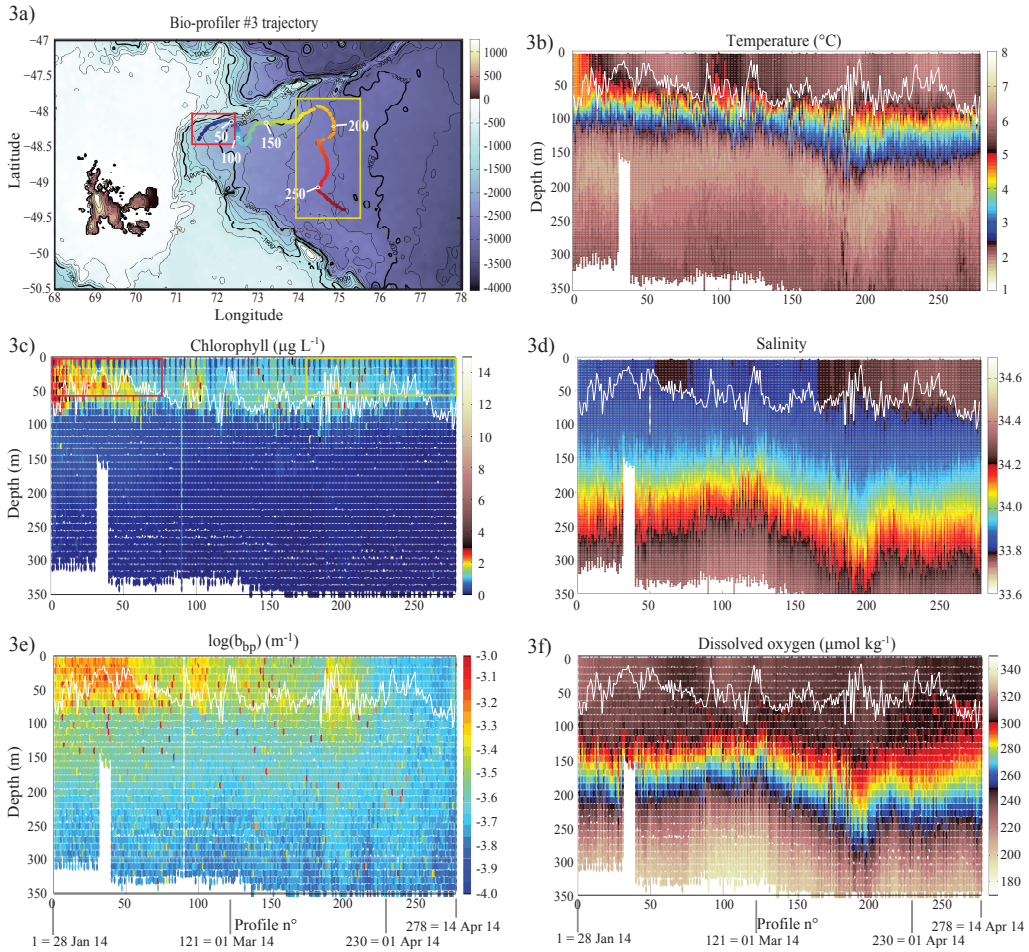

Figure 3.

BGD
11, 17413–17462, 2014

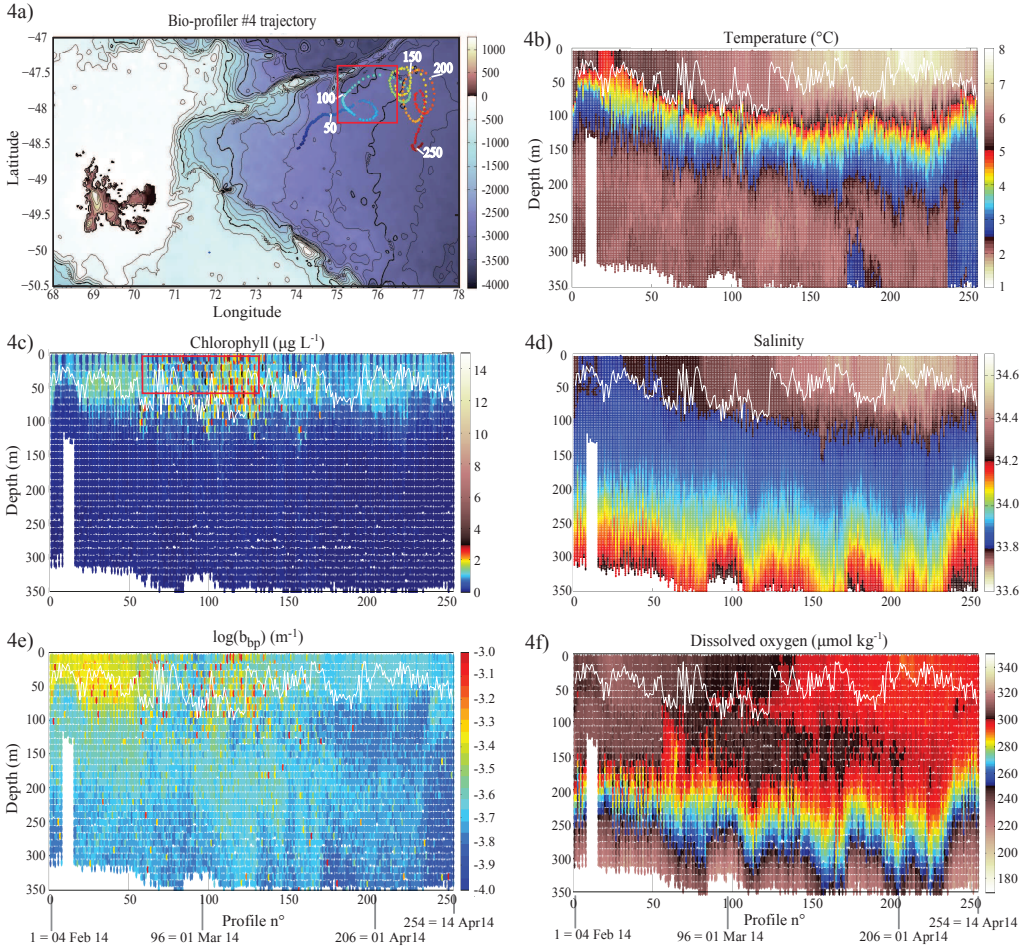

BGD
11, 17413–17462, 2014

Autonomous profiling float observations of high biomass plume

M. Grenier et al.

Figure 3. (1a) Bio-profiler #1 trajectory over the bathymetry, with each point representing a depth profile and the colour of the points changing from blue to red over time (dates are shown below the bottom plots). **(1b–1f)** Evolution of hydrological parameters along the float trajectory: **(1b)** temperature (°C), **(1c)** chlorophyll ($\mu g\,L^{-1}$), **(1d)** salinity, **(1e)** backscatter (log scale; m^{-1}), and **(1f)** dissolved oxygen ($\mu mol\,kg^{-1}$). White line represents the mixed layer depth. Red and yellow rectangles refer to rich and moderate chlorophyll areas in Fig. 6. **(2a–2f)**, **(3a–3f)**, **(4a–4f)** same as **(1a–1f)** but for bio-profiler #2, bio-profiler #3 and bio-profiler #4, respectively.

BGD
11, 17413–17462, 2014

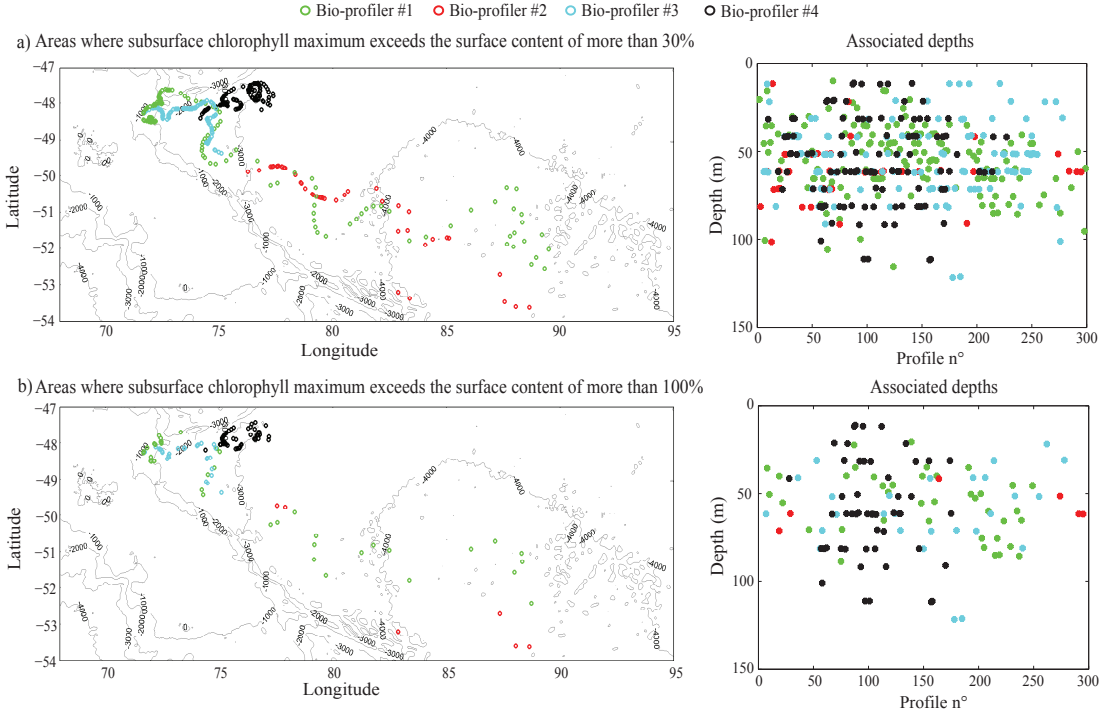

Figure 4. Locations of subsurface chlorophyll maxima. Left: areas with subsurface chlorophyll maxima exceed the surface content by more than **(a)** 30 % and **(b)** 100 %. Right: associated depths of the chlorophyll maxima.

BGD
11, 17413–17462, 2014

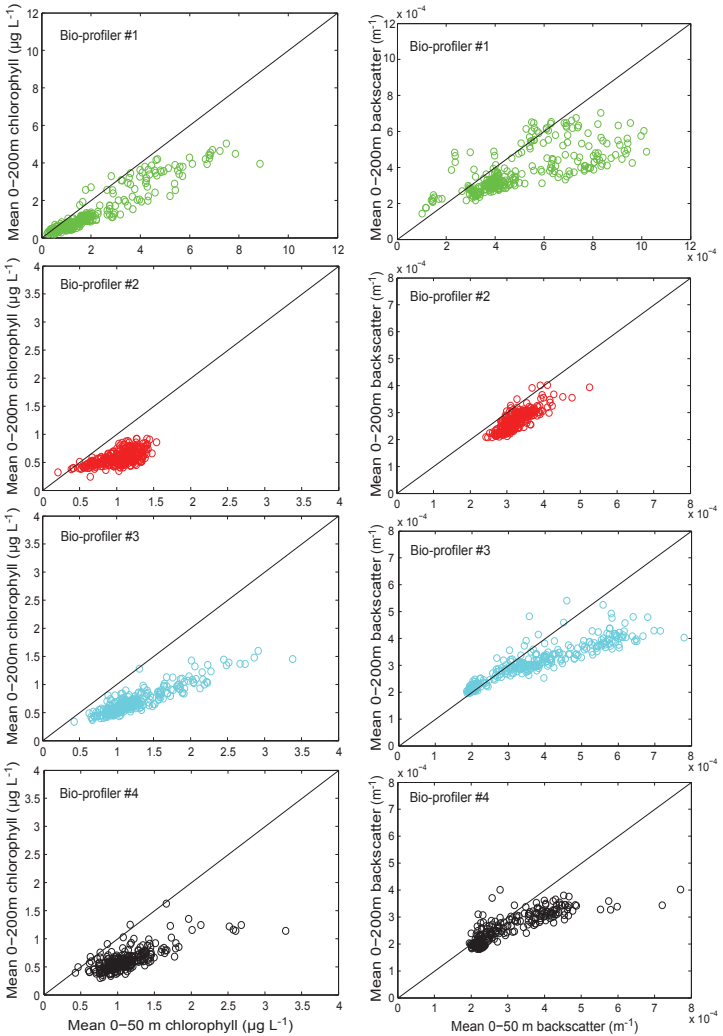

BGD
11, 17413–17462, 2014

Autonomous profiling float observations of high biomass plume

M. Grenier et al.

Figure 5. Comparison of surface (0–50 m) and water column integrated (0–200 m) biomass distributions for each bio-profiler. Left column: fluorescence phytoplankton biomass estimates. Right column: backscatter total biomass estimates (note that scales are slightly larger for bio-profiler #1 than for the others).

BGD
11, 17413–17462, 2014

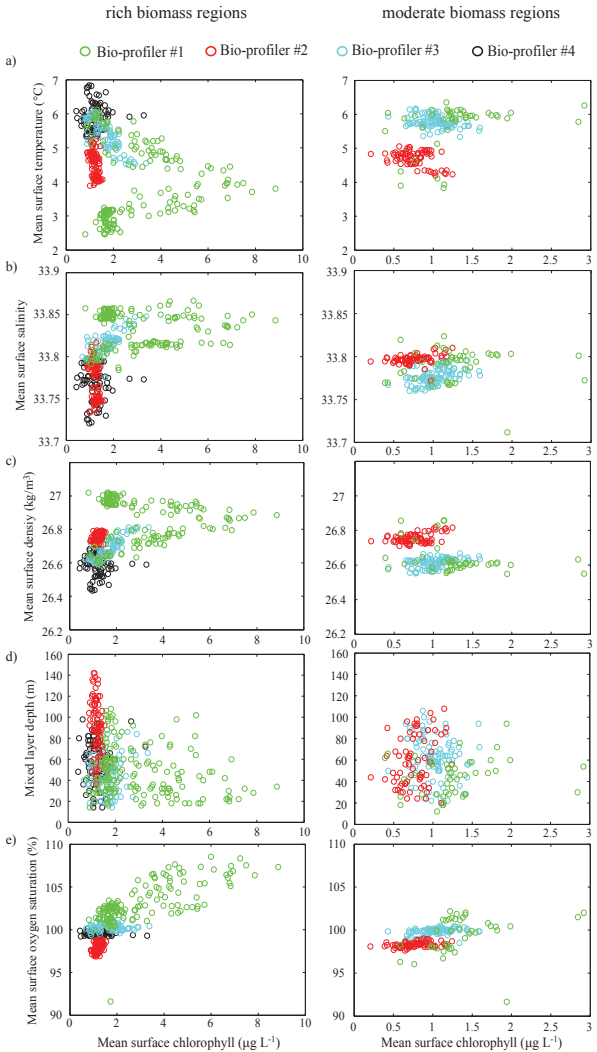

BGD
11, 17413–17462, 2014

Autonomous profiling float observations of high biomass plume

M. Grenier et al.

Figure 6. Chlorophyll relationships with surface water properties for **(a)** temperature; **(b)** salinity; **(c)** density; **(d)** mixed layer depth (MLD); **(e)** oxygen saturation state. The left column shows results for high biomass regions close to the plateau (bio-profilers #1 and #3) or entrapped in eddies (bio-profilers #2 and #4; red rectangles in Fig. 3). The right column shows results for moderate biomass regions far from the plateau (yellow rectangles in Fig. 3).

BGD
11, 17413–17462, 2014

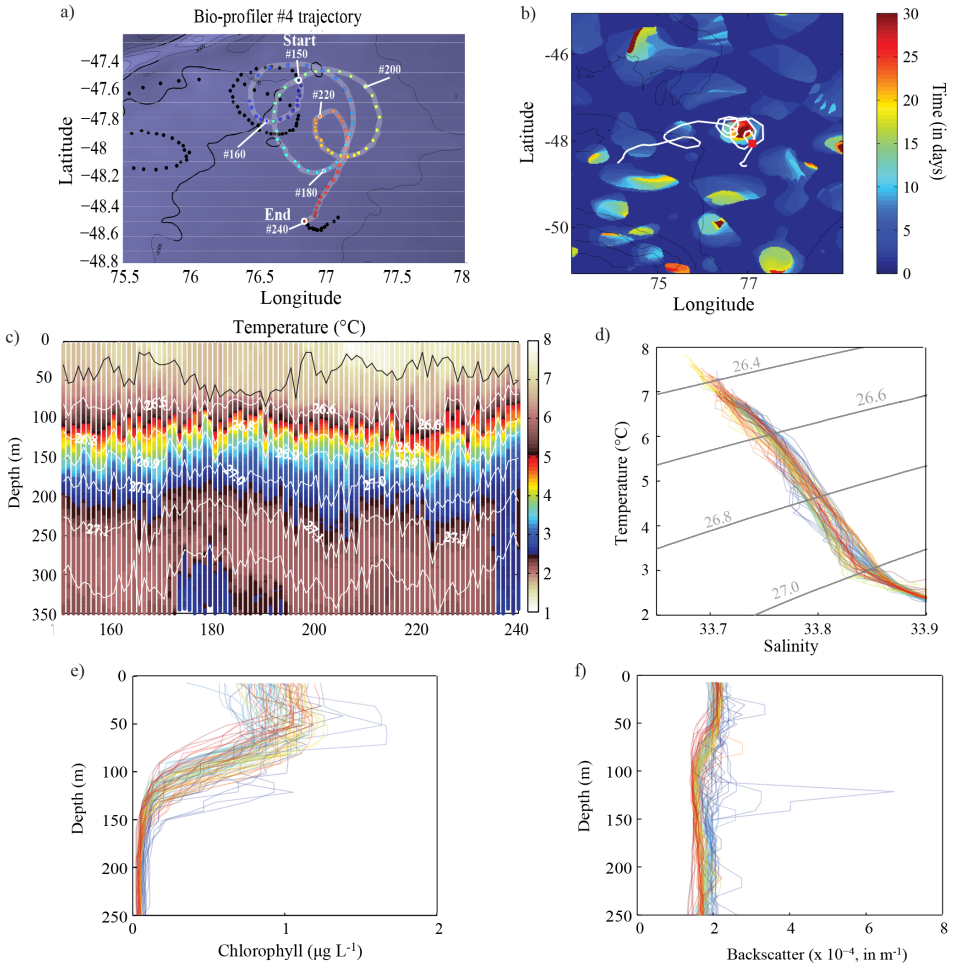

BGD
11, 17413–17462, 2014

Autonomous profiling float observations of high biomass plume

M. Grenier et al.

Figure 7. Eddy entrapment of bio-profiler #4. **(a)** Identification of entrapment along the bio-profiler trajectory, coloured by time, from blue to red. **(b)** Overlay of bio-profiler trajectory with map of eddy retention (see Methods for details of the retention calculation), relative to profile 177 (red square). A consistent sector of the trajectory is located within a long-lasting retentive structure (more than 30 days of retention). **(c)** Temperature vs. depth section with mixed layer depth (black line) and isopycnals indicated (white lines). **(d)** Temperature–salinity diagram, coloured as on the map. **(e)** Chlorophyll profiles, coloured as on the map. **(f)** Backscatter profiles, coloured as on the map. Note that chlorophyll and backscatter signals were filtered for visual clarity, using a 3 point running median.

BGD
11, 17413–17462, 2014

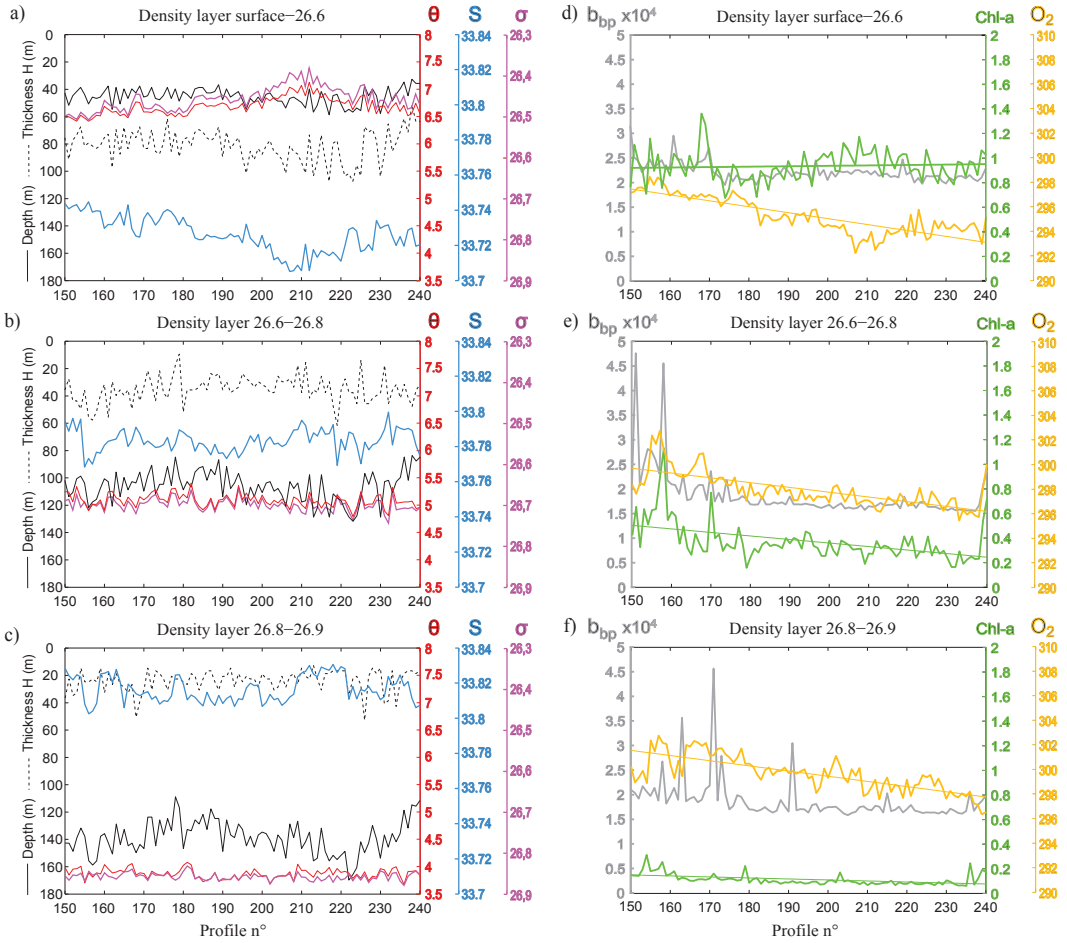

BGD
11, 17413–17462, 2014

Autonomous profiling float observations of high biomass plume

M. Grenier et al.

Figure 8. Temporal evolution during eddy entrapment for bio-profiler #4. Left: mean depth (in m; black line and scale), thickness (in m; dashed black line and black scale), temperature (θ, in $^{\circ}$C; red line and scale), salinity (S; blue line and scale) and density (σ, in kg m^{-3}; purple line and scale) as a function of profile numbers (i.e. along the eddy trajectory), for three density layers: **(d)** surface-26.6; **(e)** 26.6–26.8; **(f)** 26.8–26.9. Right: as left-side panels, but with mean chlorophyll (Chl *a*, in µg L^{-1}; green line and scale), backscatter (b_{bp}, in m^{-1}; gray line and scale), and oxygen (O_2, in µmol kg^{-1}; orange line and scale) inventories.

BGD
11, 17413–17462, 2014